Ganglion Cell-Inner Plexiform Layer Thickness of High Definition Optical Coherence Tomography in Perimetric and Preperimetric Glaucoma

Viquar U. Begum, Uday K. Addepalli, Ravi K. Yadav, Kalmuri Shankar, Sirisha Senthil, Chandra S. Garudadri, and Harsha L. Rao

VST Glaucoma Center, L V Prasad Eye Institute, Banjara Hills, Hyderabad, India

Correspondence: Harsha L. Rao, Kallam Anji Reddy campus, L V Prasad Eye Institute, Banjara Hills, Hyderabad - 500034, India; harshabl.76@gmail.com, harsha@lvpei.org.

Submitted: April 15, 2014
Accepted: June 29, 2014

Citation: Begum VU, Addepalli UK, Yadav RK, et al. Ganglion cell-inner plexiform layer thickness of high definition optical coherence tomography in perimetric and preperimetric glaucoma. *Invest Ophthalmol Vis Sci.* 2014;55:4768–4775. DOI:10.1167/iovs.14-14598

Purpose. We determined the diagnostic performance of ganglion cell-inner plexiform layer (GCIPL) parameters of high definition optical coherence tomography (HD-OCT) in perimetric and preperimetric glaucoma, and compared it to optic nerve head (ONH) and peripapillary retinal nerve fiber layer (RNFL) parameters.

Methods. In a cross-sectional study, 53 eyes of normal subjects and 83 eyes of glaucoma patients (62 perimetric and 21 preperimetric) from the Longitudinal Glaucoma Evaluation Study (LOGES) underwent HD-OCT imaging with Optic Disc and Macular Cube protocols. Diagnostic abilities of GCIPL, ONH, and RNFL parameters were determined using area under receiver operating characteristic curves (AUC) and likelihood ratios (LR).

Results. The AUCs of GCIPL parameters to diagnose perimetric glaucoma ranged from 0.84 to 0.90. The same of ONH and RNFL parameters ranged from 0.88 to 0.97 and 0.56 to 0.94, respectively. The AUCs of GCIPL, ONH, and RNFL parameters to diagnose preperimetric glaucoma ranged from 0.55 to 0.63, 0.77 to 0.92, and 0.39 to 0.80, respectively. For diagnosing preperimetric glaucoma, AUCs of all GCIPL parameters were significantly lower ($P < 0.05$) than those of the global ONH (vertical cup-to-disc ratio [CDR]; AUC, 0.92) and RNFL (average RNFL; AUC, 0.79) parameters. Outside normal limits category of GCIPL parameters also were associated with significantly smaller effects on the posttest probability of perimetric and preperimetric glaucoma.

Conclusions. The diagnostic ability of GCIPL parameters was similar to that of ONH and peripapillary RNFL parameters in perimetric glaucoma. However, in preperimetric glaucoma, the diagnostic ability of GCIPL parameters was significantly lower than that of ONH and RNFL parameters.

Keywords: glaucoma, high definition optical coherence tomography, ganglion cell/inner plexiform layer

Glaucoma, a leading cause of irreversible blindness in the world,[1] is characterized by pathological loss of retinal ganglion cells which is associated with clinically recognizable alterations in the optic nerve head (ONH) and retinal nerve fibers layer (RNFL). Imaging technologies in glaucoma, until recently, have focused predominantly on the ONH and RNFL for evaluating the structural damage in glaucoma. With the advent of spectral domain optical coherence tomography (SD-OCT), scanning the inner layers of the retina at the macula (RNFL, ganglion cell layer, and inner plexiform layer) has provided new insights into the structural damage in glaucoma and has emerged as a useful modality to diagnose glaucoma.[2–7] Cirrus high-definition OCT (HD-OCT) is one such SD-OCT device that has an algorithm called Ganglion Cell Analysis (GCA) to measure and analyze the inner retinal thickness parameters at the macula. The GCA segments out the macular RNFL layer from the ganglion cell-inner plexiform layer (GCIPL) and measures the GCIPL thicknesses separately. Recent studies with GCA have reported the diagnostic abilities of GCIPL parameters to be similar to RNFL parameters in diagnosing glaucoma.[8–14] Studies also have reported good correlation between the GCIPL parameters and the retinal sensitivities in glaucoma.[15] However, these studies were performed in patients with perimetric glaucoma and the reports on the performance of this algorithm in preperimetric glaucoma are sparse.[16,17] Also, to our knowledge, there are no studies on the diagnostic ability of this algorithm in the Indian population. The purpose of this study was to determine the diagnostic performance of GCIPL parameters in Indian eyes with perimetric and preperimetric glaucoma, and to compare it to that of ONH and peripapillary RNFL parameters.

Methods

Subjects and Protocols

This was a cross-sectional analysis of the baseline examinations of participants included in the ongoing Longitudinal Glaucoma Evaluation Study (LOGES). The LOGES is a prospective longitudinal study conducted at the L V Prasad Eye Institute, Hyderabad, India, to evaluate the structure and function in glaucoma longitudinally. Participants in LOGES include normal

subjects, patients with glaucoma, and glaucoma suspects, who are longitudinally evaluated clinically and with functional and imaging tests. Informed consent was obtained from all participants and the Ethics Committee of L V Prasad Eye Institute approved all methodology. All methods adhered to the tenets of the Declaration of Helsinki for research involving human subjects.

Inclusion criteria were age $\geq$ 18 years, best corrected visual acuity of 20/40 or better, and refractive error within $\pm$ 5 diopters (D) sphere and $\pm$ 3 D cylinder. Exclusion criteria were presence of any media opacities that prevented good quality optic disc photographs and other imaging tests, and any retinal (including macular) or neurologic disease other than glaucoma, which could confound the evaluations. All participants underwent a comprehensive ocular examination, which included a detailed medical history, best corrected visual acuity measurement, slit-lamp biomicroscopy, Goldmann applanation tonometry, gonioscopy, dilated fundus examination, visual field (VF) examination, stereoscopic optic disc photography, and SD-OCT imaging with Cirrus HD-OCT (Carl Zeiss Meditec, Inc., Dublin, CA, USA).

The VF examination was performed using a Humphrey Field analyzer, model 750i (Zeiss Humphrey Systems, Dublin, CA, USA), with the Swedish interactive threshold algorithm (SITA) standard 24-2 program. The VFs were considered reliable if the fixation losses, and false-positive and -negative response rates were less than or equal to 20%. A single observer masked to the optic disc classification, SD-OCT findings and the other eye status, graded all VFs. The VFs were classified as "glaucomatous" if the pattern SD had a *P* value of less than 5% and the glaucoma hemifield test result was outside normal limits.[18] The VFs were classified as "normal" otherwise.

Stereoscopic optic disc photographs were obtained by trained technicians using digital fundus camera (FF 450^{plus} with VISUPAC 4.2.2; Carl Zeiss Meditec Systems GmbH, Pirmasens, Germany). Photographs consisted of a 50° image centered on the optic disc, a similar image centered on the macula, a 30° image centered on the optic disc, and a 20° image centered on the disc. All these images also consisted of one colored and one red-free image each. Each optic disc photograph was evaluated independently by two of the three experts (HLR, UKA, and SS) all of whom were masked to the clinical details of the subjects and also the VF, OCT, and other eye examination results. They classified the optic discs into glaucomatous and nonglaucomatous (control) groups based on the presence or absence of characteristic glaucomatous optic disc changes (focal or diffuse neuroretinal rim thinning, localized notching, or nerve fiber layer defects). Optic discs that could not be classified definitively into glaucoma or control groups were classified as suspects. Discrepancies between the two experts were resolved by consensus.

The SD-OCT examination was performed with Cirrus HD-OCT (software version 6.0). The protocols used were Macular Cube 200 $\times$ 200 for the GCA, and Optic Disc Cube 200 $\times$ 200 for the RNFL and ONH parameters. These protocols have been explained in detail previously.[19,20] The GCA is designed to measure the GCIPL thickness within a 14.13-mm^2 elliptical annulus centered on the fovea with an inner vertical radius of 0.5 mm and outer vertical radius of 2 mm, stretched horizontally by 20%. The thickness parameters derived from GCA are the average GCIPL thickness across the entire elliptical annulus and the thickness at six 60° sectors of the elliptical annulus. The seventh parameter is the minimum GCIPL measurement determined by sampling 360 spokes of measurements extending from the center of the fovea to the edge of the ellipse in 1° intervals and selecting the spoke with the lowest average.

The ONH parameters generated by the Optic Disc Cube 200 $\times$ 200 protocol and analyzed in this study were the optic disc area, rim area, average cup-to-disc ratio (CDR), vertical CDR, and cup volume. The RNFL parameters calculated by the protocol and analyzed in this study were the average RNFL thickness (average RNFL thickness at the 3.4-mm diameter circle centered on the ONH); temporal, superior, nasal, and inferior quadrant RNFL thicknesses; and the RNFL thickness in 12 clock hours (30° segments of the measurement circle). Only good quality scans with signal strength $\geq$ 6, absence of motion and blinking artifacts, and segmentation failure were used for the analysis.

Control eyes had nonglaucomatous optic discs, as assessed by experts on disc photographs, and normal VF. Perimetric glaucoma eyes had glaucomatous optic discs and glaucomatous VF, and preperimetric glaucoma eyes had glaucomatous optic discs and normal VF results.

Statistical Analysis

Descriptive statistics included mean and SD for normally distributed variables, and median and interquartile range (IQR) for non-normally distributed variables. The Shapiro Wilk test was used to check for the normality of distribution. Receiver operating characteristic (ROC) curves were used to describe the ability of each HD-OCT software-provided parameter to discriminate perimetric and preperimetric glaucomatous eyes from control eyes. Sensitivities at fixed specificities of 80% and 95% were determined for all the parameters. To obtain confidence intervals (CIs) for area under the ROC curves (AUC), a bootstrap resampling procedure was used ($n = 1000$ resamples). As measurements from both eyes of the same subject are likely to be correlated, the standard statistical methods for parameter estimation led to underestimation of SEs and to CIs that are too narrow.[21] Therefore, the cluster of data for the study subject was considered as the unit of resampling and bias corrected SE was calculated during all estimations. This procedure has been used in the literature to adjust for the presence of multiple correlated measurements from the same unit.[22,23] The Z-test was used to compare the AUCs[24,25] and χ^2 test to compare the sensitivities at fixed specificities of HD-OCT parameters in diagnosing perimetric and preperimetric glaucoma. Likelihood ratios (LR) were reported for diagnostic categorization (outside normal limits, borderline, or within normal limits) provided after comparison with the instrument's internal normative database. The LR is the probability of a given test result in those with disease divided by the probability of the same test result in those without the disease.[26] The LR for a given test result indicates how much that result will raise or lower the probability of disease. A LR of 1 or close to 1 would mean that the test provides no additional information about the posttest probability of the disease. The LRs higher than 10 or lower than 0.1 would be associated with large effects on posttest probability, 5 to 10 or 0.1 to 0.2 with moderate effects, and 2 to 5 or 0.2 to 0.5 with small effects.[26] The 95% CIs for LRs were calculated according to the method proposed by Simel et al.[27] Statistical analyses were performed using commercial software (Stata ver. 11.2; StataCorp, College Station, TX, USA). A *P* value of $\leq$0.05 was considered statistically significant.

Results

A total of 304 eyes of 174 subjects included in LOGES had undergone macular and optic disc imaging with HD-OCT. Among these, 21 eyes of 17 subjects with poor disc photographs (5 eyes with poor quality, 12 with poor stereo,

Table 1. Age, VF and HD-OCT Features of the Study Participants

	Control Group, 53 Eyes	Preperimetric Glaucoma, 21 Eyes	Perimetric Glaucoma, 62 Eyes	*P* Value*	*P* Value†
Age, y	42 (33, 53)	47 (36, 60)	53 (45, 58)	0.46	0.02
Spherical equivalent, D	0 (−0.50, 0.75)	0 (0, 1.25)	0 (−0.75, 0.50)	0.33	0.76
IOP, mm Hg	15 (13, 17)	15 (13, 18)	17 (14, 20)	0.61	0.01
Mean deviation, dB	−2.0 (−3.1, −0.7)	−1.9 (−2.9, −0.8)	−11.4 (−17.5, −4.9)	0.86	<0.001
Pattern SD, dB	1.7 (1.4, 2.1)	1.7 (1.3, 1.9)	7.6 (4.9, 10.0)	0.50	<0.001
VF index, %	99 (97, 100)	99 (98, 100)	75 (56, 89)	0.54	<0.001
ONH parameters					
Signal strength	6 (6, 7)	6 (6, 7)	6 (6, 7)	0.79	0.17
Disc area, mm^2	2.2 (2.0, 2.5)	2.4 (1.9, 2.5)	2.0 (1.8, 2.5)	0.95	0.13
Rim area, mm^2	1.2 (1.1, 1.4)	0.9 (0.8, 1.1)	0.7 (0.5, 0.9)	<0.001	<0.001
Average CDR	0.66 (0.61, 0.71)	0.78 (0.73, 0.81)	0.83 (0.77, 0.88)	<0.001	<0.001
Vertical CDR	0.64 (0.59, 0.67)	0.76 (0.73, 0.81)	0.85 (0.77, 0.88)	<0.001	<0.001
Cup volume, mm^3	0.34 (0.22,0.46)	0.53 (0.40, 0.85)	0.79 (0.58, 1.13)	<0.001	<0.001
RNFL parameters					
Clock hour_1, μm	106 (92, 123)	86 (77, 96)	70 (53, 87)	<0.001	<0.001
Clock hour_2, μm	89 (73, 105)	81 (74, 91)	64 (56, 76)	0.08	<0.001
Clock hour_3, μm	58 (52, 67)	59 (47, 69)	53 (48, 58)	0.58	0.004
Clock hour_4, μm	65 (54, 74)	65 (55, 71)	57 (50, 63)	0.43	<0.001
Clock hour_5, μm	97 (83, 113)	77 (72, 93)	63 (52, 74)	0.003	<0.001
Clock hour_6, μm	131 (114, 150)	108 (97, 136)	66 (51, 91)	0.003	<0.001
Clock hour_7, μm	126 (108, 142)	106 (101, 115)	58 (48, 84)	<0.001	<0.001
Clock hour_8, μm	60 (52, 67)	62 (58, 72)	49 (42, 57)	0.16	<0.001
Clock hour_9, μm	47 (42, 52)	48 (41, 57)	45 (39, 53)	0.51	0.26
Clock hour_10, μm	72 (62, 78)	64 (55, 73)	53 (44, 61)	0.04	<0.001
Clock hour_11, μm	116 (101, 131)	98 (82, 108)	67 (55, 96)	0.008	<0.001
Clock hour_12, μm	118 (107, 136)	91 (79, 108)	75 (60, 96)	<0.001	<0.001
Temporal quadrant, μm	60 (53, 66)	60 (54, 65)	49 (42, 55)	0.79	<0.001
Superior quadrant, μm	116 (106, 125)	87 (83, 105)	68 (58, 90)	<0.001	<0.001
Nasal quadrant, μm	71 (65, 79)	69 (56, 74)	58 (52, 65)	0.22	<0.001
Inferior quadrant, μm	119 (110, 130)	102 (87, 110)	62 (51, 84)	<0.001	<0.001
Average thickness, μm	94 (85, 98)	80 (72, 86)	61 (52, 71)	<0.001	<0.001
GCIPL parameters					
Signal strength	7 (6, 8)	6 (6, 7)	7 (6, 8)	0.12	0.63
Superotemporal quadrant, μm	79 (71, 83)	75 (72, 80)	62 (51, 72)	0.13	<0.001
Superior quadrant, μm	81 (75, 87)	79 (69, 82)	62 (53, 74)	0.06	<0.001
Superonasal quadrant, μm	84 (77, 89)	81 (75, 87)	70 (58, 79)	0.36	<0.001
Inferonasal quadrant, μm	84 (77, 88)	81 (75, 86)	66 (58, 76)	0.17	<0.001
Inferior quadrant, μm	80 (75, 85)	77 (72, 81)	59 (53, 67)	0.18	<0.001
Inferotemporal quadrant, μm	79 (75, 85)	76 (74, 83)	56 (50, 66)	0.18	<0.001
Average, μm	81 (76, 86)	78 (75, 82)	64 (55, 72)	0.17	<0.001
Minimum, μm	78 (68, 82)	75 (70, 77)	49 (45, 60)	0.34	<0.001

All values represent median (with IQR in parentheses).
* Represents the *P* value associated with the comparison between control and preperimetric glaucoma group.
† Represents the *P* value associated with the comparison between control and perimetric glaucoma group.

and 4 with poor quality and stereo) and 62 eyes classified as optic disc suspects were excluded from the analysis. A further 28 eyes with unreliable VFs were excluded. Of the remaining 193 eyes eligible for the analysis, 57 with poor quality HD-OCT scans (18 eyes with poor quality optic disc and macular scans, 27 with poor quality disc scans, and 12 with poor quality macular scans) were excluded, leaving behind 53 eyes of 38 control subjects (21 men), 21 eyes of 18 patients (12 men) with preperimetric glaucoma, and 62 eyes of 46 patients (34 men) with perimetric glaucoma for the final analysis. Table 1 shows the age, refractive error, IOP, and VF characteristics of the three groups of subjects on the day of imaging with HD-OCT. Perimetric glaucoma patients were significantly older than control subjects. Therefore, the AUCs and sensitivities at fixed specificities of HD-OCT parameters were calculated after adjusting for the difference in age between perimetric glaucoma and control groups using covariate-adjustment as proposed by Pepe.[28] The ONH, RNFL, and GCIPL parameters of the three groups of subjects also are shown in Table 1. Disc area of the subjects and the signal strengths of optic disc and macular scans were comparable among the three groups. All the ONH, RNFL, and GCIPL parameters were significantly different between the control and perimetric glaucoma groups. while all of the ONH, but none of the GCIPL parameters were significantly different between the control and preperimetric glaucoma groups. Among the RNFL parameters, average, inferior, and superior quadrant RNFL measurements and the clock hour measurements in inferior and superior quadrants were significantly different between the control and preperimetric glaucoma groups. Age, refractive error, optic disc area, and signal strength of the scans were comparable between the perimetric and preperimetric glaucoma groups, while all VF

Table 2. The AUC and Sensitivities at Fixed Specificities (With 95% CIs in Parentheses) of the HD-OCT Parameters to Diagnose Perimetric Glaucoma and Preperimetric Glaucoma

	Perimetric Glaucoma			Preperimetric Glaucoma		
	AUC	Sensitivity at 95% Specificity	Sensitivity at 80% Specificity	AUC	Sensitivity at 95% Specificity	Sensitivity at 80% Specificity
ONG parameters						
Rim area	0.95 (0.89–0.98)	76% (56–92)	92% (81–98)	0.85 (0.73–0.93)	48% (16–79)	71% (42–95)
Average CDR	0.93 (0.87–0.97)	81% (63–91)	89% (78–97)	0.85 (0.73–0.94)	52% (22–76)	71% (42–92)
Vertical CDR	0.97 (0.93–0.99)	85% (70–93)	94% (84–100)	0.92 (0.82–0.99)	76% (48–100)	90% (67–100)
Cup volume	0.88 (0.79–0.94)	56% (30–75)	74% (53–85)	0.77 (0.61–0.88)	38% (11–63)	48% (10–70)
RNFL parameters						
Clock hour_1	0.86 (0.77–0.93)	56% (32–73)	77% (60–90)	0.74 (0.60–0.87)	14% (4–36)	57% (29–88)
Clock hour_2	0.83 (0.72–0.90)	37% (9–58)	61% (34–84)	0.62 (0.45–0.75)	10% (3–21)	14% (4–35)
Clock hour_3	0.67 (0.54–0.79)	6% (1–15)	40% (18–71)	0.53 (0.35–0.69)	19% (5–47)	33% (10–54)
Clock hour_4	0.67 (0.53–0.78)	11% (3–38)	29% (6–56)	0.55 (0.38–0.69)	10% (4–22)	19% (5–37)
Clock hour_5	0.85 (0.76–0.92)	34% (2–65)	77% (60–91)	0.72 (0.58–0.84)	27% (13–50)	53% (40–71)
Clock hour_6	0.92 (0.85–0.96)	81% (61–92)	84% (72–93)	0.72 (0.54–0.86)	33% (4–63)	62% (40–94)
Clock hour_7	0.94 (0.88–0.98)	76% (60–89)	90% (79–97)	0.75 (0.62–0.85)	14% (4–36)	43% (11–75)
Clock hour_8	0.76 (0.65–0.86)	39% (19–60)	65% (48–83)	0.39 (0.25–0.54)	0%	0%
Clock hour_9	0.56 (0.44–0.69)	21% (3–40)	34% (15–48)	0.44 (0.26–0.60)	14% (4–29)	29% (9–50)
Clock hour_10	0.83 (0.74–0.90)	44% (16–74)	76% (59–89)	0.65 (0.50–0.77)	14% (4–38)	29% (8–50)
Clock hour_11	0.86 (0.77–0.92)	56% (20–72)	73% (49–83)	0.69 (0.54–0.83)	19% (5–50)	48% (22–73)
Clock hour_12	0.84 (0.74–0.91)	52% (24–75)	76% (58–89)	0.78 (0.64–0.89)	19% (5–42)	57% (19–89)
Temporal quadrant	0.78 (0.66–0.87)	40% (8–66)	65% (48–80)	0.50 (0.35–0.62)	5% (3–10)	19% (4–37)
Superior quadrant	0.89 (0.80–0.94)	56% (32–72)	82% (70–91)	0.79 (0.64–0.91)	10% (3–55)	71% (43–91)
Nasal quadrant	0.79 (0.66–0.89)	27% (7–70)	63% (21–79)	0.58 (0.40–0.74)	14% (4–35)	29% (6–47)
Inferior quadrant	0.94 (0.87–0.98)	81% (62–94)	90% (78–97)	0.80 (0.64–0.90)	38% (9–67)	57% (25–84)
Average thickness	0.93 (0.86–0.97)	74% (43–89)	89% (77–98)	0.79 (0.64–0.88)	24% (4–40)	57% (21–84)
GCIPL parameters						
Superotemporal quadrant	0.87 (0.79–0.93)	60% (43–75)	73% (58–89)	0.60 (0.42–0.76)	14% (4–38)	24% (5–60)
Superior quadrant	0.87 (0.79–0.93)	55% (37–70)	74% (56–87)	0.63 (0.44–0.75)	5% (3–6)	33% (6–52)
Superonasal quadrant	0.84 (0.74–0.92)	42% (23–64)	63% (39–80)	0.55 (0.38–0.71)	5% (3–6)	14% (4–38)
Inferonasal quadrant	0.88 (0.77–0.94)	32% (16–63)	74% (40–89)	0.58 (0.40–0.73)	0%	24% (5–52)
Inferior quadrant	0.90 (0.83–0.96)	55% (34–67)	82% (65–93)	0.58 (0.40–0.73)	0%	24% (5–52)
Inferotemporal quadrant	0.90 (0.82–0.96)	69% (39–82)	79% (62–88)	0.58 (0.40–0.73)	5% (3–8)	24% (5–52)
Average	0.90 (0.82–0.95)	55% (33–75)	79% (57–91)	0.59 (0.43–0.74)	5% (3–6)	24% (5–52)
Minimum	0.90 (0.81–0.95)	61% (3–78)	82% (68–93)	0.56 (0.42–0.70)	5% (3–11)	24% (4–50)

and OCT parameters were significantly lesser in the perimetric compared to the preperimetric glaucoma group.

The AUCs and sensitivities at fixed specificities of the ONH, RNFL, and GCIPL parameters to differentiate perimetric and preperimetric glaucoma from control eyes are shown in Table 2. Among the ONH parameters, vertical CDR, rim area, and average CDR showed the best AUCs to diagnose perimetric and preperimetric glaucoma. Among the RNFL parameters, inferior quadrant and average RNFL parameters showed the best AUCs to diagnose perimetric and preperimetric glaucoma. Among the GCIPL parameters, inferior, inferotemporal, average, and minimum GCIPL thickness parameters showed the best AUCs to diagnose perimetric glaucoma, while the superior and superotemporal GCIPL parameters showed the best AUCs to diagnose preperimetric glaucoma. The same parameters also showed the best sensitivities at fixed specificities of 80% and 95% to diagnose perimetric and preperimetric glaucoma. However, AUC of no one GCIPL parameter was statistically significantly better than that of the others ($P > 0.1$ for AUC comparison among GCIPL parameters) either in diagnosing perimetric or preperimetric glaucoma.

Table 3 shows the *P* values associated with the difference in the AUCs and sensitivities at 95% specificity of global and quadrant measurements of ONH, RNFL, and GCIPL parameters.

Table 3. The Difference and *P* Values Associated With the Difference (in Parentheses) in the Diagnostic Ability Parameters Between the Global and Quadrant Measurements of Different Scanning Locations of HD-OCT

	Perimetric Glaucoma		Preperimetric Glaucoma	
	AUC	Sensitivity at 95% Specificity	AUC	Sensitivity at 95% Specificity
Vertical CDR vs. average RNFL	0.04 (0.15)	11% (0.20)	0.13 (0.01)	52% (0.002)
Vertical CDR vs. average GCIPL	0.07 (0.04)	30% (0.001)	0.33 (<0.001)	71% (<0.001)
Average RNFL vs. average GCIPL	0.03 (0.27)	19% (0.04)	0.20 (<0.001)	19% (0.19)
Superior RNFL vs. superior GCIPL	0.02 (0.62)	1% (0.94)	0.16 (0.02)	5% (0.98)
Inferior RNFL vs. inferior GCIPL	0.04 (0.17)	26% (0.004)	0.22 (0.001)	38% (0.006)

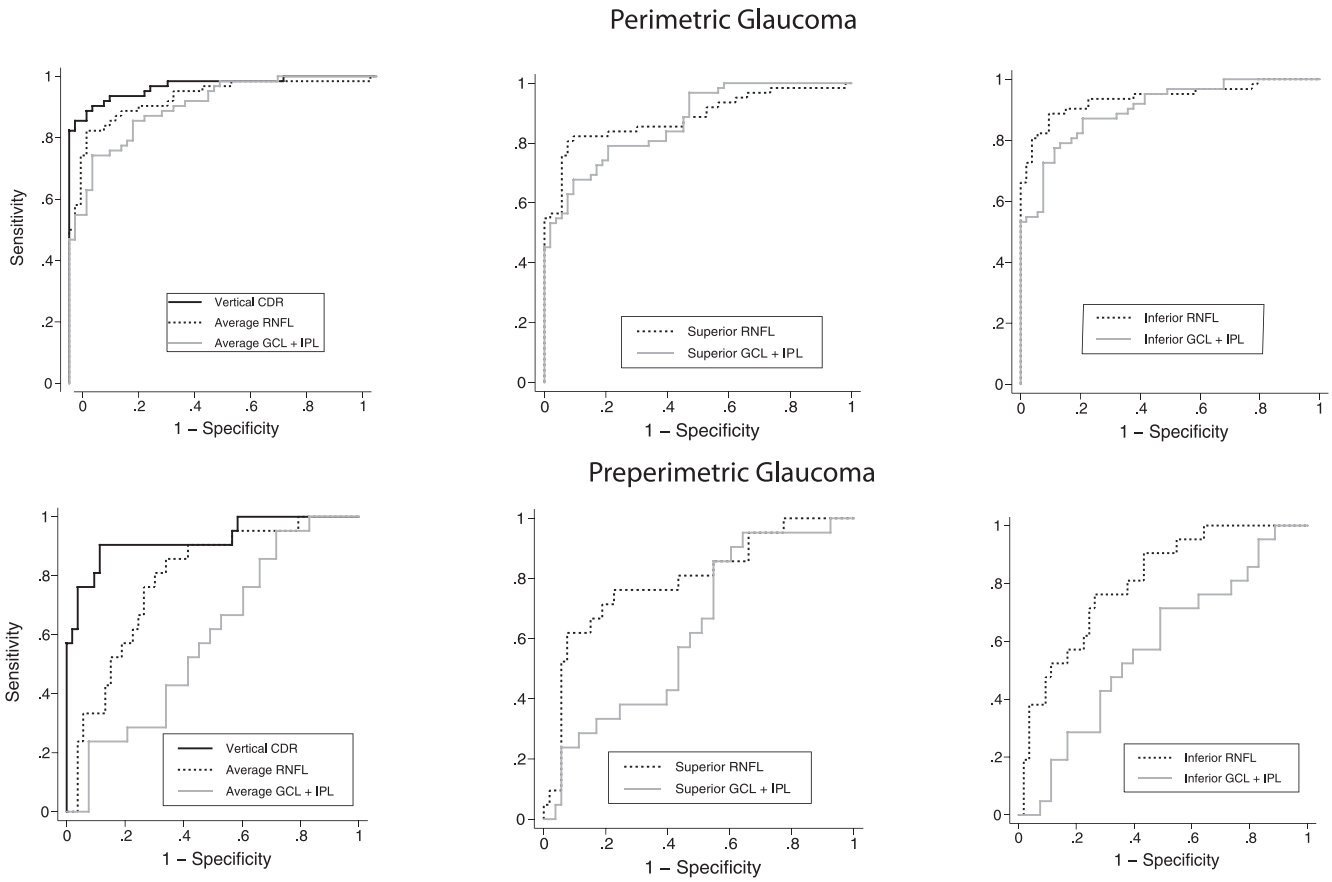

Figure. The ROC curves of global and quadrant measurements of different scanning locations of HD-OCT in perimetric (*top row*) and preperimetric (*bottom row*) glaucoma. GCL, ganglion cell layer; IPL, inner plexiform layer.

For diagnosing perimetric glaucoma, AUC of vertical CDR was significantly better than average GCIPL thickness. Sensitivities at 95% specificity of vertical CDR and average RNFL thickness were significantly better than that of average GCIPL parameter. For diagnosing preperimetric glaucoma, AUCs of all GCIPL parameters were significantly lower than those of vertical CDR and average RNFL parameters. Sensitivity at 95% specificity of vertical CDR was significantly better than that of average RNFL and average GCIPL parameters. The Figure shows the ROC curves of global and quadrant measurements of ONH, RNFL, and GCIPL parameters in diagnosing perimetric (top row) and preperimetric (bottom row) glaucoma.

Table 4 shows the LRs associated with the normative database classification of HD-OCT parameters to discriminate perimetric and preperimetric glaucoma from control eyes. Outside normal limits category of all ONH parameters, and the superior, inferior, and average RNFL parameters were associated with large effects on the posttest probability of perimetric glaucoma, while the same of GCIPL parameters were associated with moderate effects. Within normal limits category of all HD-OCT parameters was associated with large to moderate effects on the posttest probability of perimetric glaucoma. Outside normal limits category of all ONH parameters was associated with large effects on the posttest probability of preperimetric glaucoma. Outside normal limits category of superior, inferior, and average RNFL parameters was associated with moderate effects, while the same of GCIPL parameters was associated with no effects on the posttest probability of preperimetric glaucoma. Within normal limits category of all ONH parameters was associated with small effects, while that of RNFL and GCIPL parameters was associated with no effect on the posttest probability of preperimetric glaucoma.

In clinical practice, glaucoma is suspected when an abnormal test result on imaging is found with any of the ONH, RNFL, or GCIPL parameters (or-logic criterion) and an eye is considered healthy when an abnormal result is not found with any of these parameters (and-logic criterion). Therefore, we also evaluated the LRs for the above logic criteria. For diagnosing perimetric glaucoma, the positive and negative LRs were 2.3 (1.6–3.2) and 0.0 (0.0–0.2), respectively. For diagnosing preperimetric glaucoma, the same were 1.9 (1.3–2.8) and 0.3 (0.1–0.9), respectively.

Discussion

In this study to evaluate the diagnostic performance of GCIPL parameters in glaucoma, we found that the AUCs of GCIPL parameters were good and comparable to those of ONH and peripapillary RNFL parameters in perimetric glaucoma. With a median MD of −11.4 dB, our perimetric glaucoma group consisted predominantly of eyes with moderate-to-severe glaucoma. Our results are similar to that of previous studies evaluating GCIPL parameters in moderate-to-severe glaucoma.[9,11] However, when we compared the sensitivities at fixed specificities, we found that the sensitivity at 95% specificity of vertical CDR and average RNFL was significantly better than that of average GCIPL parameter. When we evaluated the GCIPL parameters in preperimetric glaucoma, the AUCs of GCIPL parameters were significantly lower than those of ONH and RNFL parameters. Sensitivities at 95% specificity also were

Table 4. LRs (With 95% CI) of the Normative Database Classification of HD-OCT Parameters to Discriminate Perimetric and Preperimetric Glaucoma From Control Eyes

	Perimetric Glaucoma			Preperimetric Glaucoma		
	WNL	Borderline	ONL	WNL	Borderline	ONL
ONH parameters						
Rim area	0.1 (0.0–0.2)	0.4 (0.1–1.6)	16.2 (4.2–62.4)	0.4 (0.2–0.8)	1.7 (0.5–5.1)	11.3 (2.8–46.1)
Average CDR	0.1 (0.0–0.2)	0.5 (0.2–1.8)	10.8 (3.7–31.9)	0.3 (0.1–0.8)	2.1 (0.7–5.9)	8.2 (2.6–25.8)
Vertical CDR	0.1 (0.0–0.2)	0.3 (0.1–1.3)	31.8 (4.6–220)	0.2 (0.1–0.7)	2.1 (0.7–5.9)	27.8 (4.0–196)
Cup volume	0.2 (0.1–0.3)	2.5 (0.5–11.7)	32.6 (4.7–226)	0.5 (0.3–0.9)	5.0 (1.0–24.6)	19.0 (2.5–143)
RNFL parameters						
Clock hour_1	0.4 (0.3–0.6)	6.0 (1.4–25.2)	28.7 (4.1–203)	0.8 (0.7–1.0)	6.3 (1.3–30.0)	9.6 (1.1–85.6)
Clock hour_2	1.0 (0.9–1.0)	4.6 (1.4–14.9)	3.3 (0.1–78.0)	0.9 (0.8–1.1)	1.7 (0.3–9.5)	7.7 (0.3–180)
Clock hour_3	1.0 (0.9–1.1)	NA	1.3 (0.2–7.5)	1.0 (0.9–1.1)	NA	1.5 (0.1–15.3)
Clock hour_4	NA	3.4 (0.8–15.3)	NA	NA	2.5 (0.4–16.6)	NA
Clock hour_5	0.5 (0.3–0.7)	5.6 (1.3–23.5)	9.4 (3.0–28.9)	1.0 (0.9–1.1)	5.0 (1.0–25.5)	1.0 (0.1–9.0)
Clock hour_6	0.2 (0.1–0.4)	1.4 (0.4–5.7)	38.6 (5.5–270)	0.9 (0.7–1.1)	2.5 (0.5–11.4)	8.3 (0.9–75.1)
Clock hour_7	0.3 (0.2–0.4)	1.1 (0.3–4.9)	37.1 (5.3–260)	0.9 (0.8–1.1)	1.7 (0.3–9.3)	5.3 (0.5–54.7)
Clock hour_8	0.8 (0.7–0.9)	NA	9.7 (1.3–74.1)	1.0 (0.9–1.1)	NA	0.8 (0.0–19.3)
Clock hour_9	1.0 (0.9–1.1)	NA	1.9 (0.4–9.9)	1.0 (0.9–1.1)	NA	0.6 (0.0–11.3)
Clock hour_10	0.6 (0.5–0.8)	NA	5.9 (2.2–16.0)	1.0 (0.9–1.2)	NA	0.8 (0.1–6.9)
Clock hour_11	0.4 (0.3–0.5)	1.0 (0.4–2.5)	29.8 (4.3–209)	0.9 (0.8–1.1)	2.9 (1.2–6.9)	3.5 (0.2–52.8)
Clock hour_12	0.6 (0.5–0.8)	2.6 (0.9–7.5)	19.6 (2.7–140)	1.0 (0.8–1.1)	3.8 (1.2–12.1)	3.3 (0.2–49.1)
Temporal quadrant	0.7 (0.6–0.9)	12.0 (1.6–88.0)	7.6 (1.8–31.6)	1.0 (0.9–1.1)	NA	1.2 (0.1–12.9)
Superior quadrant	0.2 (0.1–0.4)	3.0 (0.6–13.8)	13.6 (4.5–41.1)	0.5 (0.3–0.8)	3.8 (0.7–21.0)	8.5 (2.6–28.0)
Nasal quadrant	1.0 (0.9–1.0)	4.7 (1.1–20.3)	5.0 (0.2–102)	0.9 (0.8–1.1)	3.8 (0.7–21.0)	8.2 (0.3–193)
Inferior quadrant	0.2 (0.1–0.3)	0.6 (0.1–3.3)	20.8 (5.3–81.4)	0.7 (0.5–0.9)	1.7 (0.3–9.3)	9.2 (2.1–40.5)
Average RNFL	0.2 (0.1–0.3)	0.9 (0.1–5.8)	13.6 (4.5–41.1)	0.7 (0.5–1.0)	2.5 (0.4–16.7)	5.4 (1.5–19.3)
GCIPL parameters						
Superotemporal quadrant	0.3 (0.2–0.5)	3.4 (0.4–29.7)	3.5 (2.0–6.1)	0.9 (0.7–1.3)	5.0 (0.5–52.8)	1.2 (0.5–3.1)
Superior quadrant	0.4 (0.3–0.6)	0.9 (0.2–3.2)	4.5 (2.2–9.1)	0.9 (0.6–1.2)	1.3 (0.2–6.4)	1.8 (0.7–5.1)
Superonasal quadrant	0.6 (0.4–0.7)	0.4 (0.1–1.4)	7.3 (2.4–22.4)	1.0 (0.8–1.1)	0.4 (0.1–2.8)	1.5 (0.3–8.5)
Inferonasal quadrant	0.5 (0.4–0.7)	1.4 (0.4–5.7)	8.8 (2.9–27.0)	1.0 (0.9–1.2)	2.5 (0.6–11.5)	0.9 (0.1–8.3)
Inferior quadrant, μm	0.3 (0.2–0.4)	NA	5.7 (2.8–11.6)	0.9 (0.7–1.2)	NA	1.4 (0.5–4.4)
Inferotemporal quadrant	0.2 (0.1–0.4)	0.2 (0.0–1.4)	7.6 (3.3–17.5)	0.9 (0.7–1.1)	0.5 (0.1–4.0)	1.9 (0.6–6.4)
Average	0.3 (0.2–0.5)	1.7 (0.5–6.5)	5.4 (2.7–10.8)	0.9 (0.7–1.2)	NA	1.7 (0.6–4.8)
Minimum	0.1 (0.1–0.3)	0.4 (0.1–1.2)	5.5 (2.8–11.0)	1.0 (0.7–1.2)	0.3 (0.0–2.1)	1.3 (0.4–3.8)

Analysis was based on number of eyes. NA, indeterminate; WNL, within normal limits; ONL, outside normal limits.

lower than those of ONH and RNFL parameters. Peripapillary RNFL is expected to be better than GCIPL in diagnosing early glaucoma because of two reasons. First is that the sampling that happens with GCA of HD-OCT only considers the ganglion cells at the macula. Though macula has the highest density of ganglion cells, macular region (as measured by the elliptical annulus of the HD-OCT) constitutes only 50% of the total ganglion cells in the retina. Therefore, any ganglion cell damage outside the measurement annulus is not detected by the algorithm. In contrast to this, peripapillary RNFL evaluates the axons of all ganglion cells of the retina. Therefore, the pickup rate for ganglion cell damage is expected to be better with peripapillary RNFL compared to GCIPL parameters. Second reason for the above finding is the inherent bias in favor of the RNFL and disc parameters, and against the macular parameters introduced because of the design of the study. The gold standard definition of glaucoma in our study and in all other similar studies evaluating the diagnostic ability of macular parameters is based on the optic nerve and RNFL changes evaluated by the experts and not on macular changes. This is because the glaucomatous changes at macula, unlike the changes at ONH and RNFL, are not detectable clinically. Such a bias is known to inflate the diagnostic abilities of ONH and RNFL parameters.[29] The ONH parameters performed better than RNFL parameters in diagnosing perimetric and preperimetric glaucoma. This probably is because of the bias introduced in the selection of control group, which consisted of optic discs with no suspicious findings of glaucoma. We have discussed this in greater detail in a previous publication.[30]

Studies evaluating GCIPL parameters of Cirrus HD-OCT in preperimetric glaucoma are sparse.[16,17] Both these studies, one by Sung et al.[16] and the other by Kim et al.,[17] done in Korean population, in contrast to our results, found that the GCIPL parameters were as good as the ONH and the RNFL parameters in diagnosing preperimetric glaucoma. One of the possible reasons for the greater diagnostic abilities of GCIPL parameters in the Korean population may be the location of glaucomatous damage being closer to the fovea. Earlier studies have shown a higher prevalence of normal tension glaucoma in the Korean population[31] with glaucomatous damage closer to fixation.[32] Kim et al.,[17] in fact, found that the diagnostic ability of GCIPL parameters increased significantly if the RNFL defects were closer to the fovea.

We also found that the AUC of no one GCIPL parameter was better than that of the others either in diagnosing perimetric or preperimetric glaucoma. There was no preferential affection of any particular GCIPL sector or parameter. This is in contrast to the previous studies that have found the inferior, inferotemporal, and minimum GCIPL sectors to be the ones showing thinning and, therefore, better AUCs and sensitivities to

diagnose perimetric and preperimetric glaucoma.[8–13,17] Nasal sector GCIPL thickness parameters had significantly lower diagnostic performance in all these studies. This is in accordance with the fact that the nasal GCIPL sectors, which correspond to the papillomacular bundle, are more resistant to glaucomatous damage. However, the reason for not finding such a pattern of damage in our study is not clear.

In addition to sensitivity, specificity, and AUC, diagnostic tests also are summarized in terms of LR, which is higher than the previous measures in hierarchy, as it expresses the magnitude by which the probability of a diagnosis in a given patient is modified by the results of the test.[33,34] In other words, the LR indicates how much a given diagnostic test result will raise or lower the pretest probability of the disease in question. Therefore, we evaluated the LRs associated with the diagnostic categorization of SD-OCT parameters. The magnitude of the LRs associated with the diagnostic categorization of HD-OCT parameters in the perimetric glaucoma and normal groups were similar to that reported in a recent study by Mwanza et al.[14] in early perimetric glaucoma. However, when we evaluated the same in preperimetric glaucoma, we found that the outside normal limits category of ONH, RNFL, and GCIPL parameters were, respectively, associated with large, moderate, and no effects on the posttest probability of preperimetric glaucoma. It is important to note that these effects, though small, still can become relevant and useful, depending on other clinical information and the pretest probability of disease. It also is important to note that the internal normative database of Cirrus HD-OCT predominantly consists of Caucasian subjects and, therefore, might be less relevant to the Indian population.

Most diagnostic studies in glaucoma have employed a case-control design similar to the one used in our study, including glaucoma patients (cases), defined based on the presence of characteristic glaucomatous optic disc and RNFL changes with or without VF defects; and normal subjects (controls), usually recruited from the general population. However, in clinical practice, a diagnostic test is used to detect disease in subjects suspected of having disease and not in subjects with either clear-cut evidence of the disease or with no suspicious findings of the disease. Multiple studies have evaluated the bias introduced in such situations.[6,30,35] Therefore, caution should be exercised when interpreting estimates of diagnostic ability provided in our study. These estimates should not be extrapolated to the situation of detecting disease in glaucoma suspects. Preperimetric glaucoma in our study was diagnosed based on a single evaluation of the disc photographs by experts. There is a possibility of a few optic discs diagnosed as preperimetric glaucoma actually being normal physiological variants. This is, however, less likely as two experts independently classified the optic discs as glaucomatous. Optic discs that could not be classified definitively into glaucoma or control groups were classified as suspects and excluded from the analysis. Medeiros et al.,[36] therefore, have recommended longitudinal evaluation of optic discs for detecting change and definitively diagnosing preperimetric glaucoma. In a more recent study, Medeiros et al.[37] also have shown that progressive rim area loss was highly predictive of the development of VF loss in glaucoma. Longitudinal investigations using HD-OCT in LOGES should be able to clarify its role as a complementary diagnostic test to be used in clinical practice. The other limitation of our study was the small sample size, especially in the preperimetric glaucoma group. We had to exclude a significant number of eyes because of bad quality HD-OCT images (57/193). When we evaluated the subjects who had to be excluded because of bad quality OCT images, we found that they were significantly ($P = 0.01$) older (median age = 56 years) than the ones included (median age = 48 years). Possibility of our study results being biased due to this must be kept in mind.

In the present study, we analyzed a large number of parameters available from the three different scanning areas of Cirrus HD-OCT. The large number of analyses may have increased the chance of a type I error during hypothesis testing. Several methods have been proposed in the statistics literature to potentially correct for multiple comparisons, but there is no consensus on whether they should be applied routinely and what specific method should be used.[38,39] Although we did not apply methods to correct for multiple comparisons, it is important to emphasize that some of the differences detected in our study may have occurred just by chance and also could be specific to the sample used in our investigation.

In conclusion, diagnostic ability of GCIPL parameters obtained with GCA was similar to that of the ONH and peripapillary RNFL parameters in perimetric glaucoma. However, in preperimetric glaucoma, the diagnostic ability of GCIPL parameters was significantly lower than that of the ONH and RNFL parameters.

Acknowledgments

Supported by Hyderabad Eye Research Foundation.

Disclosure: **V.U. Begum**, None; **U.K. Addepalli**, None; **R.K. Yadav**, None; **K. Shankar**, None; **S. Senthil**, None; **C.S. Garudadri**, Optovue (F), Allergan (C), Alcon (C), Merck (C); **H.L. Rao**, Allergan (C)

References

1. Quigley HA, Broman AT. The number of people with glaucoma worldwide in 2010 and 2020. *Br J Ophthalmol*. 2006;90:262–267.
2. Tan O, Chopra V, Lu AT, et al. Detection of macular ganglion cell loss in glaucoma by Fourier-domain optical coherence tomography. *Ophthalmology*. 2009;116:2305–2314.
3. Rao HL, Babu GJ, Sekhar GC. Comparison of the diagnostic capability of the Heidelberg retina tomographs 2 and 3 for glaucoma in the Indian population. *Ophthalmology*. 2010;117:275–281.
4. Rao HL, Babu JG, Addepalli UK, Senthil S, Garudadri CS. Retinal nerve fiber layer and macular inner retina measurements by spectral domain optical coherence tomograph in Indian eyes with early glaucoma. *Eye (Lond)*. 2012;26:133–139.
5. Arintawati P, Sone T, Akita T, Tanaka J, Kiuchi Y. The applicability of ganglion cell complex parameters determined from SD-OCT images to detect glaucomatous eyes. *J Glaucoma*. 2013;22:713–718.
6. Rao HL, Addepalli UK, Chaudhary S, et al. Ability of different scanning protocols of spectral domain optical coherence tomography to diagnose preperimetric glaucoma. *Invest Ophthalmol Vis Sci*. 2013;54:7252–7257.
7. Na JH, Lee K, Lee JR, Baek S, Yoo SJ, Kook MS. Detection of macular ganglion cell loss in preperimetric glaucoma patients with localized retinal nerve fibre defects by spectral-domain optical coherence tomography. *Clin Exp Ophthalmol*. 2013;41:870–880.
8. Mwanza JC, Durbin MK, Budenz DL, et al. Glaucoma diagnostic accuracy of ganglion cell-inner plexiform layer thickness: comparison with nerve fiber layer and optic nerve head. *Ophthalmology*. 2012;119:1151–1158.
9. Takayama K, Hangai M, Durbin M, et al. A novel method to detect local ganglion cell loss in early glaucoma using spectral-domain optical coherence tomography. *Invest Ophthalmol Vis Sci*. 2012;53:6904–6913.

10. Kotowski J, Folio LS, Wollstein G, et al. Glaucoma discrimination of segmented cirrus spectral domain optical coherence tomography (SD-OCT) macular scans. *Br J Ophthalmol*. 2012; 96:1420–1425.
11. Jeoung JW, Choi YJ, Park KH, Kim DM. Macular ganglion cell imaging study: glaucoma diagnostic accuracy of spectral-domain optical coherence tomography. *Invest Ophthalmol Vis Sci*. 2013;54:4422–4429.
12. Akashi A, Kanamori A, Nakamura M, Fujihara M, Yamada Y, Negi A. Comparative assessment for the ability of Cirrus, RTVue, and 3D-OCT to diagnose glaucoma. *Invest Ophthalmol Vis Sci*. 2013;54:4478–4484.
13. Nouri-Mahdavi K, Nowroozizadeh S, Nassiri N, et al. Macular ganglion cell/inner plexiform layer measurements by spectral domain optical coherence tomography for detection of early glaucoma and comparison to retinal nerve fiber layer measurements. *Am J Ophthalmol*. 2013;156:1297–1307.
14. Mwanza JC, Budenz DL, Godfrey DG, et al. Diagnostic performance of optical coherence tomography ganglion cell-inner plexiform layer thickness measurements in early glaucoma. *Ophthalmology*. 2014;121:849–854.
15. Sato S, Hirooka K, Baba T, Tenkumo K, Nitta E, Shiraga F. Correlation between the ganglion cell-inner plexiform layer thickness measured with cirrus HD-OCT and macular visual field sensitivity measured with microperimetry. *Invest Ophthalmol Vis Sci*. 2013;54:3046–3051.
16. Sung MS, Yoon JH, Park SW. Diagnostic validity of macular ganglion cell-inner plexiform layer thickness deviation map algorithm using Cirrus HD-OCT in preperimetric and early glaucoma [published online ahead of print November 14, 2013]. *J Glaucoma*.
17. Kim MJ, Jeoung JW, Park KH, Choi YJ, Kim DM. Topographic profiles of retinal nerve fiber layer defects affect the diagnostic performance of macular scans in preperimetric glaucoma. *Invest Ophthalmol Vis Sci*. 2014;55:2079–2087.
18. Anderson DR, Patella VM. *Automated Static Perimetry*. 2nd ed. St. Louis, MO: Mosby; 1999:152.
19. Mwanza JC, Oakley JD, Budenz DL, Anderson DR. Ability of cirrus HD-OCT optic nerve head parameters to discriminate normal from glaucomatous eyes. *Ophthalmology*. 2011;118: 241–248.
20. Mwanza JC, Oakley JD, Budenz DL, Chang RT, Knight OJ, Feuer WJ. Macular ganglion cell-inner plexiform layer: automated detection and thickness reproducibility with spectral domain-optical coherence tomography in glaucoma. *Invest Ophthalmol Vis Sci*. 2011;52:8323–8329.
21. Glynn RJ, Rosner B. Accounting for the correlation between fellow eyes in regression analysis. *Arch Ophthalmol*. 1992; 110:381–387.
22. Zhou XH, Obuchowski NA, McClish DK. Analysis of correlated ROC data. In: Zhou XH, Obuchowski NA, McClish DK, eds. *Statistical Methods in Diagnostic Medicine*. New York, NY: John Wiley & Sons, Inc.;2002:274–306.
23. Alonzo TA, Pepe MS. Distribution-free ROC analysis using binary regression techniques. *Biostatistics*. 2002;3:421–432.
24. Zhou XH, Obuchowski NA, McClish DK. Comparing the accuracy of two diagnostic tests. In: Zhou XH, Obuchowski NA, McClish DK, eds. *Statistical Methods in Diagnostic Medicine*. New York, NY: John Wiley & Sons; 2002:165–194.
25. DeLong ER, DeLong DM, Clarke-Pearson DL. Comparing the areas under two or more correlated receiver operating characteristic curves: a nonparametric approach. *Biometrics*. 1988;44:837–845.
26. Jaeschke R, Guyatt GH, Sackett DL. Users' guides to the medical literature. III. How to use an article about a diagnostic test. B. What are the results and will they help me in caring for my patients? The Evidence-Based Medicine Working Group. *JAMA*. 1994;271:703–707.
27. Simel DL, Samsa GP, Matchar DB. Likelihood ratios with confidence: sample size estimation for diagnostic test studies. *J Clin Epidemiol*. 1991;44:763–770.
28. Pepe MS. *The Statistical Evaluation of Medical Tests for Classification and Prediction*. Oxford, UK: Oxford University Press; 2003:130–167.
29. Garway-Heath DF, Hitchings RA. Sources of bias in studies of optic disc and retinal nerve fibre layer morphology. *Br J Ophthalmol*. 1998;82:986.
30. Rao HL, Kumbar T, Addepalli UK, et al. Effect of spectrum bias on the diagnostic accuracy of spectral-domain optical coherence tomography in glaucoma. *Invest Ophthalmol Vis Sci*. 2012;53:1058–1065.
31. Kim CS, Seong GJ, Lee NH, Song KC, Namil Study Group KGS. Prevalence of primary open-angle glaucoma in central South Korea the Namil study. *Ophthalmology*. 2011;118:1024–1030.
32. Kim DM, Seo JH, Kim SH, Hwang SS. Comparison of localized retinal nerve fiber layer defects between a low-teen intraocular pressure group and a high-teen intraocular pressure group in normal-tension glaucoma patients. *J Glaucoma*. 2007;16:293–296.
33. Langlotz CP. Fundamental measures of diagnostic examination performance: usefulness for clinical decision making and research. *Radiology*. 2003;228:3–9.
34. Medeiros FA, Zangwill LM, Bowd C, Weinreb RN. Comparison of the GDx VCC scanning laser polarimeter, HRT II confocal scanning laser ophthalmoscope, and stratus OCT optical coherence tomograph for the detection of glaucoma. *Arch Ophthalmol*. 2004;122:827–837.
35. Medeiros FA, Ng D, Zangwill LM, Sample PA, Bowd C, Weinreb RN. The effects of study design and spectrum bias on the evaluation of diagnostic accuracy of confocal scanning laser ophthalmoscopy in glaucoma. *Invest Ophthalmol Vis Sci*. 2007;48:214–222.
36. Medeiros FA, Zangwill LM, Bowd C, Sample PA, Weinreb RN. Use of progressive glaucomatous optic disk change as the reference standard for evaluation of diagnostic tests in glaucoma. *Am J Ophthalmol*. 2005;139:1010–1018.
37. Medeiros FA, Lisboa R, Zangwill LM, et al. Evaluation of progressive neuroretinal rim loss as a surrogate end point for development of visual field loss in glaucoma. *Ophthalmology*. 2014;121:100–109.
38. Savitz DA, Olshan AF. Multiple comparisons and related issues in the interpretation of epidemiologic data. *Am J Epidemiol*. 1995;142:904–908.
39. Sankoh AJ, Huque MF, Dubey SD. Some comments on frequently used multiple endpoint adjustment methods in clinical trials. *Stat Med*. 1997;16:2529–2542.

Investigative Ophthalmology & Visual Science